PRAMANA
— journal of
physics

Vol. 75, No. 5
November 2010
pp. 769–785

High average power supercontinuum sources

J C TRAVERS
Femtosecond Optics Group, Department of Physics, Imperial College London,
Prince Consort Road, London, SW7 2AZ, UK
E-mail: john.travers03@imperial.ac.uk

Abstract. The physical mechanisms and basic experimental techniques for the creation of high average spectral power supercontinuum sources is briefly reviewed. We focus on the use of high-power ytterbium-doped fibre lasers as pump sources, and the use of highly nonlinear photonic crystal fibres as the nonlinear medium. The most common experimental arrangements are described, including both continuous wave fibre laser systems with over 100 W pump power, and picosecond mode-locked, master oscillator power fibre amplifier systems, with over 10 kW peak pump power. These systems can produce broadband supercontinua with over 50 and 1 mW/nm average spectral power, respectively. Techniques for numerical modelling of the supercontinuum sources are presented and used to illustrate some supercontinuum dynamics. Some recent experimental results are presented.

Keywords. Supercontinuum generation; fibre lasers; nonlinear fibre optics; photonic crystal fibre; modulation instability; optical solitons.

PACS Nos 42.65.Ky; 42.55.Wd; 42.81.Dp; 42.65.Sf

1. Introduction

High average spectral power supercontinuum sources are useful for a wide range of applications because of a number of favourable properties:

- Extremely broad spectral widths, often over 1000 nm, and even spanning the whole transparency region of silica glass fibre (0.3–2.4 μm) from the ultraviolet (UV) to the mid-infrared [1–3] (and into the mid-infrared for fluoride glass fibres [4]).
- High spatial coherence, directionality and brightness, similar to a laser source.
- Potentially very high spectral power, often over 1 mW/nm for modulation instability-based systems, and over 50 mW/nm has been demonstrated [5].
- Potentially high temporal coherence, allowing for pulse compression and high accuracy metrology.

Essentially, supercontinuum sources can possess the broad bandwidth of thermal sources, such as sunlight, but many of the desirable properties of lasers. This has lead some to use the term 'sunlight laser' to describe supercontinuum sources.

Supercontinuum generation is also of great interest for studying the dynamics of nonlinear systems in general, and some connections have been made to rogue or freak oceanic waves [6–10], Hawking radiation [11] and thermodynamics [12].

There are several broad classes of supercontinuum generation depending on both the pump and fibre parameters:

Pumping in the normal dispersion regime. In this case the dynamics are mostly restricted to two effects, self-phase modulation (SPM) and Raman scattering. Raman scattering dominates for long pulses (around 100 ps or longer), leading to a cascade of discrete Raman Stokes lines. Self-phase modulation dominates for shorter pump pulses with sufficient power. In the latter case, a supercontinuum can be produced for sufficiently short and powerful pump conditions, and it usually has very good coherence properties, useful in metrology for example, or for subsequent pulse compression.

Low-order soliton pumping in the anomalous dispersion regime. For pumping with pulses, which approximately correspond to optical solitons of low effective order (approximately $N < 15$ [13,14], see eq. (9)), soliton fission will dominate. This corresponds to the common case of ultra-short pump pulses (around 100 fs) with several kilowatts peak power. This often leads to a coherent supercontinuum. However, average power scaling is limited to significantly increasing the repetition rate of the pump laser system.

High-power, long pulse pumping in the anomalous dispersion regime. For continuous wave (CW) or relatively long pump pulses (around 1 ps or longer, although this actually depends on the effective soliton order: $N > 15$ [13,14]), we are in the modulation stability regime. This usually corresponds to pumping with very high-order solitons (often $N > 500$). This can lead to exceptionally broad supercontinua with very high average power and spectral flatness, but they will lack temporal coherence.

Of course, this analysis is oversimplified, and the transitions between the various regimes are continuous. A complete analysis, including detailed numerical modelling, is usually required to fully understand the dominant supercontinuum mechanisms.

In what follows, I look at only the high power pumping in the modulation instability regime. This leads to the highest average spectral powers achieved to date. In this brief review I concentrate mostly on important practical aspects for designing, modelling and constructing supercontinuum sources. Detailed descriptions of the nonlinear dynamics can be found elsewhere, such as the classic reference books [15–18], and review papers [13,14,19,20].

Section 2 describes common experimental arrangements for constructing supercontinuum sources. Section 3 describes the most common technique for numerical modelling of supercontinuum generation. Section 4 describes a number of design choices for particular supercontinuum outputs. Finally, §5 describes some recent experimental results.

2. Experimental arrangements

In this section I broadly and qualitatively describe guidelines for the construction of supercontinuum sources. The usual experimental set-up for supercontinuum generation with a fibre-based source is shown in figure 1. The fibre pump source may pass through an isolator (ISO) to prevent back reflections into any power amplifier stages and then into the chosen nonlinear fibres used for supercontinuum generation. Usually the pump source will be directly spliced to the nonlinear supercontinuum fibres, which are often photonic crystal fibres. Three supercontinuum fibre arrangements are shown, as discussed in §§4 and 5. In the next sections I describe possible pump source configurations and the choice of fibres.

2.1 *Pump systems*

For fibre laser based pump systems, average powers of the order of 10 W can be achieved with picosecond master oscillators, and power fibre amplifier (MOPFA) configurations. Significantly, higher average powers are much harder to obtain because of pulse energy limitations, and can mostly be achieved through repetition rate scaling [21]. Instead, continuous wave pump systems can be used, allowing average power scaling beyond the level of 100 W, although with significantly reduced peak power. In what follows I look at these two systems. I look specifically at ytterbium-doped fibre systems which operate around 1070 nm, but most of the discussion also applies to other gain materials.

Figure 2a shows the set-up for a picosecond MOPFA system. The master oscillator is a mode-locked fibre laser, which has been shown to be compact and robust short pulse sources [22]. The saturable absorber is often a semiconductor saturable absorber (SESAM) [23], although carbon nanotubes are recent competitive alternatives [24,25]. The Bragg grating can be chirped, to compensate for the normal dispersion of ytterbium-doped fibre and thus allow operation in the soliton regime, although this is not essential for subsequent supercontinuum generation. One power fibre amplifier stage is shown, although one or more pre-amplifiers may

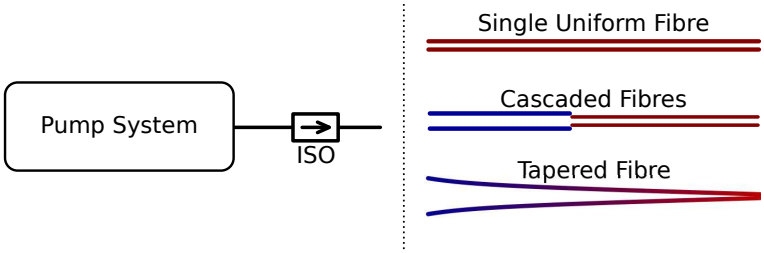

Figure 1. The general experimental set-up for supercontinuum generation. The fibre coupled pump source may pass through an isolator (ISO) to prevent back reflections into any power amplifier stages and then into the nonlinear fibres used for supercontinuum generation. Usually the pump source will be directly spliced to the nonlinear supercontinuum fibres, which are often photonic crystal fibres. Three supercontinuum fibre arrangements are shown, as discussed in the text.

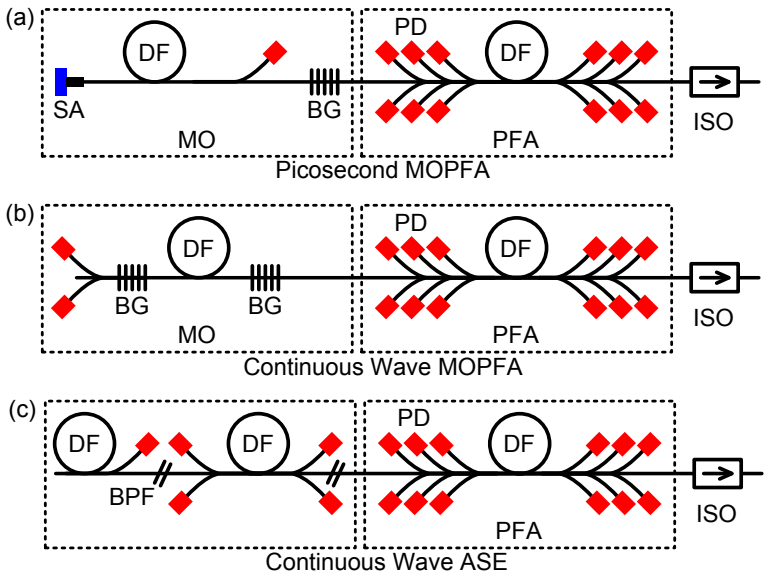

Figure 2. Experimental set-ups for (**a**) picosecond MOPFA, (**b**) continuous wave MOPFA and (**c**) continuous wave ASE source. PD – pump diode, DF – doped fibre, BG – Bragg grating, SA – saturable absorber, ISO – isolator, BPF – band pass filter, MO – master oscillator, PFA – power fibre amplifier.

also be included to minimize amplified spontaneous emission (ASE). Such a master oscillator will commonly produce ∼5 ps pulses at ∼50 MHz with a few milliwatts average power, although these parameters can vary significantly depending on the exact set-up. After the amplification stages average powers of ∼10 W are typical, although higher powers are achievable [21]. Sources such as this have been the most successful for generating high average power supercontinua with extreme spectral widths, spanning from the ultraviolet (0.3 μm) to the infrared (2.4 μm) [1–3].

Figure 2b shows the set-up for a continuous wave fibre laser-based MOPFA. Here, the first stage is a simple CW fibre laser, producing a few watts of pump power and the subsequent fibre amplifier (or chain of amplifiers) can produce several hundreds of watts of average power. It should be noted that the pump linewidth may broaden due to nonlinear coupling between the longitudinal modes of the oscillator and amplifier stages and hence the output may show significant, random, intensity and phase fluctuations. Optimal control of such fluctuations can significantly enhance the supercontinuum [26,27]. Alternatively, an amplified spontaneous emission (ASE) source may be constructed as in figure 2c. In this case, the forward ASE of a chain of amplifiers is filtered and further amplified, and hence a continuous wave source may be achieved which does not contain longitudinal modes and may have lower noise properties [28]. Both of these systems can produce output powers greater than 100 W.

All these systems are fully fibre integrated, ensuring robust and stable operation. The output isolators are not essential, but makes the system considerably more stable against back reflection causing oscillation of the power amplifier and potential

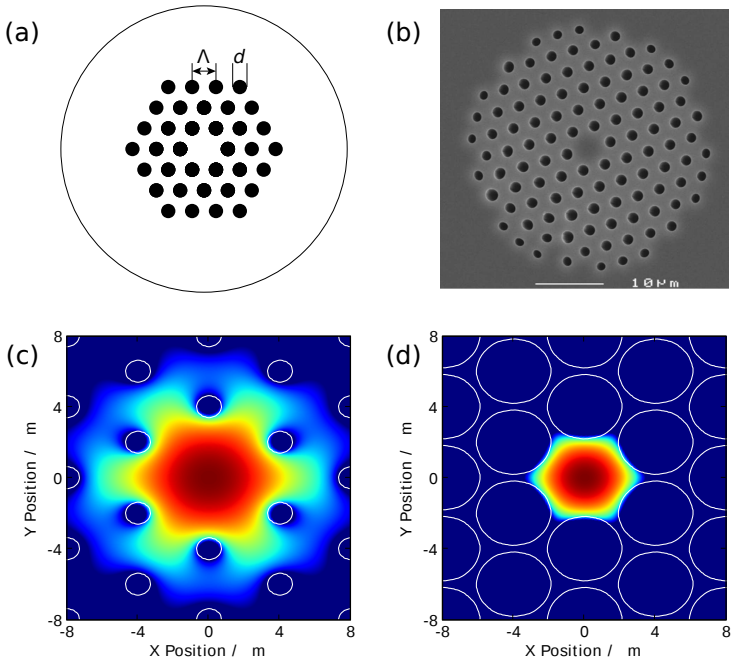

Figure 3. Photonic crystal fibre structures. (**a**) Definition of the PCF parameters; (**b**) an SEM image of a PCF (fibre F1 described below); (**c**) and (**d**) the mode pattern of light at a wavelength of 1070 nm in a PCF with $\Lambda = 3$ μm and for (**c**) $d/\Lambda = 0.3$, and for (**d**) $d/\Lambda = 0.9$.

damage to upstream components. Individual stages are also often isolated. The fibre output after the final isolator may be spliced to fibres with the particular nonlinear and dispersive properties suitable for supercontinuum generation. These fibres will typically have significantly different mode field diameters as they usually require smaller core sizes to achieve higher intensities and hence larger nonlinear coefficients. Splicing to such fibres may require intermediate fibres to match the mode field diameters. Often these will be fibres with a high germanium concentration in the core which, when heated, disperses towards the cladding and enlarges the mode field diameter. In this way one end can be spliced quickly to the small core nonlinear fibre, ensuring good mode coupling, whereas the other end is heated for a prolonged time to enlarge the mode to match that at the fibre output of the pump system [5,29]. In addition, it may be important to strip any light excited into the cladding or coating of the fibre using index-matched optical glue, to prevent burning [5,29].

2.2 *Photonic crystal fibre*

Photonic crystal fibre (PCF) [30–33] allows for enormous control over the dispersive properties of the fibre, because of the strong, but easily controllable contribution to dispersion from the waveguide [34–36]. A solid core, index guiding PCF structure

can be defined by the pitch (air-hole to air-hole spacing) Λ, and the air-hole diameter relative to the pitch d/Λ, as shown in figure 3a and illustrated in a scanning electron micrograph (SEM) of a PCF, as shown in figure 3b. By varying these parameters, fibres with a very wide range of dispersion curves can be created [34–36]. In addition, PCFs can be designed to have extremely small core areas and tight mode confinement [37]. Both of these properties are due to the strong variation in light confinement of PCFs, as illustrated in figures 3c and d which shows how light at the same wavelength of 1070 nm has very different confinement based on variation of the d/Λ parameters. Combined, these properties allow for a careful choice of optimal parameters for supercontinuum generation. A number of design choices along with modelling results will be discussed in §4.

3. Modelling

Photonic crystal fibres have such a wide range of parameter choices that optimal fibre design for a given pump source and supercontinuum output will require a number of iteractions to refine, however, their manufacture is costly and time consuming. In contrast, numerical simulations are low-cost, convenient and invaluable, as they provide the equivalent of perfect experimental diagnostics in an ideal laboratory environment, and allow this design process to occur far quicker than experiment alone, although experiments must always be performed to verify the results. In this section I describe the main techniques used for simulating supercontinuum source.

3.1 *Model*

The propagation of an electromagnetic wave travelling through an optical fibre, as for any medium, can be described by Maxwell's equations, from which a wave equation can be derived. A number of different derivations are described in [13,38–41]. The equation used in what follows most closely corresponds to the results in [41].

We define our propagation equation in terms of a linearly polarized, complex spectral envelope $\tilde{E}(z,\Omega)$, where z is the axial distance along the fibre and $\Omega = \omega - \omega_0$ is the angular frequency with respect to our chosen reference frequency ω_0. In this form, we assume that the transverse field profile is defined by a constant fibre mode shape, which can be factored out of the propagation dynamics into two constants, the fibre propagation constant $\beta(\omega)$, corresponding to an eigenvalue of Maxwell's equations for the transverse fibre structure, and the effective area A_{eff} defined by integrating over the corresponding eigenvector. A time-domain envelope can be obtained from this via a Fourier transform defined by

$$E(z,t) = \mathcal{F}^{-1}\{\tilde{E}(z,\Omega)\} = \frac{1}{2\pi}\int_{-\infty}^{\infty} \tilde{E}(z,\Omega)\exp[-i(\Omega)t]\mathrm{d}\omega. \tag{1}$$

We define the field envelope amplitude such that $|E(z,t)|^2$ gives the instantaneous power in watts. The propagation equation for $\tilde{E}(z,\Omega)$ is then [41]

$$\partial_z \tilde{E}' = i\bar{\gamma}(\omega)\exp(-i\hat{L}(\omega)z) \times \mathcal{F}\left\{\bar{E}(z,t)\int_{-\infty}^{\infty} R(t')|\bar{E}(z,t-t')|^2 d\,\mathrm{d}t'\right\}, \tag{2}$$

with the variable changes:

$$\bar{E}(z,t) = \mathcal{F}^{-1}\left\{\frac{\tilde{E}(z,\omega)}{A_{\mathrm{eff}}^{1/4}(\omega)}\right\}, \tag{3}$$

and

$$\tilde{E}'(z,\Omega) = \tilde{E}(z,\Omega)\exp(-i\hat{L}(\omega)z). \tag{4}$$

In these equations, $\hat{L}(\omega)$ is the linear operator, given by $\hat{L}(\omega) = \beta(\omega) - \beta(\omega_0) - \beta_1(\omega_0)\Omega + i\alpha(\omega)/2$ and $n_{\mathrm{eff}}(\omega) = c\beta(\omega)/\omega$ is the effective index of the mode. β_n are the nth derivatives of β with respect to ω and $\alpha(\omega)$ is the power attenuation (or gain) coefficient. The frequency-dependent nonlinear coefficient is defined as

$$\bar{\gamma}(\omega) = \frac{n_2 n_0 \omega}{c n_{\mathrm{eff}}(\omega) A_{\mathrm{eff}}^{1/4}(\omega)}, \tag{5}$$

where n_0 is the linear refractive index at ω_0 and n_2 is the nonlinear refractive index given by $n_2 = 3\chi^{(3)}/(4\epsilon_0 c n_0^2)$, with $\chi^{(3)}$ the third-order susceptibility of the medium and ϵ_0 the vacuum permittivity. The electronic contribution to n_2 can be regarded as instantaneous for pulse durations longer than ∼10 fs. The Raman contribution, however, is delayed. It is usual to account for this by writing a delayed nonlinear response function [42–44]:

$$R(t) = (1 - f_{\mathrm{r}})\delta(t) + f_{\mathrm{r}} h_{\mathrm{r}}(t), \tag{6}$$

where $h_{\mathrm{r}}(t)$ is the time-domain Raman response, derived from the frequency-domain Raman response ($h_{\mathrm{r}}(\omega)$) by a Fourier transform. The frequency response itself is usually determined from measurements of the Raman gain cross-section and the Kramers–Kronig relations [42]. I use the analytic version described in [43]. The integral of $h_{\mathrm{r}}(t)$ over all time is normalized to unity. $f_{\mathrm{r}} \sim 0.18$ is the fractional Raman contribution to n_2.

The effective area, A_{eff}, can be defined a number of ways. In conventional optical fibres, with low index and nonlinearity contrast between the core and cladding, the scalar definition is commonly used [15], but in PCFs with high refractive index contrast, and significant proportions of the field propagating in air, a full vectorial calculation of the effective area is required [45].

If we ignore the frequency dependence of the effective area and index, then $\bar{\gamma}(\omega)$ is reduced to the conventional nonlinear coefficient:

$$\gamma(\omega_0) = \frac{n_2 n_0 \omega_0}{c n_{\mathrm{eff}}(\omega_0) A_{\mathrm{eff}}(\omega_0)}. \tag{7}$$

Equation (2) is a version of the generalized nonlinear Schrödinger equation. It can be reduced to the more conventional time-domain nonlinear Schrödinger equation, by ignoring the frequency dependence of the effective area, effective mode

index and attenuation coefficient, and performing an inverse Fourier transform. If we then neglect the dispersion of the nonlinearity, the delayed nonlinearity (Raman term), higher-order dispersion and attenuation, we recover the conventional nonlinear Schrödinger equation which can be analytically solved for the soliton solutions [46].

Solitons play a very important role in modulation instability-based supercontinuum generation. The envelope field of a soliton is given by

$$E_{\mathrm{sol}}(z,t) = \sqrt{P_0}\,\mathrm{sech}\left(\frac{t}{\tau_0}\right)\exp\left(iz\frac{\beta_2}{2\tau_0^2}\right), \tag{8}$$

where P_0 is the soliton power and τ_0 is the soliton duration. The soliton power, P_0, is given by

$$N^2 = \frac{\gamma P_0 \tau_0^2}{|\beta_2|}, \tag{9}$$

where the integer N is the soliton order. For $N = 1$ the soliton is said to be fundamental. If the soliton propagates through a taper, or shifts due to Raman self-scattering [47,48], then it may adiabatically broaden or compress in order to maintain its shape if the local dispersion or nonlinearity varies; in such cases the duration will follow:

$$\tau_0 \propto \frac{|\beta_2|}{\gamma}. \tag{10}$$

3.2 *Numerical solution*

The propagation constants and mode profiles can be calculated by a wide range of methods for solving Maxwell's equations, including beam propagation, finite element and finite difference solvers. I use the plane-wave expansion method, through the free software package MIT Photonic Bands [49]. Many other methods are available, as reviewed in [36].

Equation (2) can be integrated directly in the frequency domain using most ordinary differential equation solvers, such as the Runge–Kutta method. The Raman convolutions can be efficiently computed using the convolution theorem and fast Fourier transform. Some example codes for solving eq. (2) are given in [50].

Although the spectrum and temporal intensity profile, as they evolve through the fibre, are extremely useful, a far better understanding of the very complex supercontinuum dynamics can be obtained from studying the field spectrograms. These allow the association of processes simultaneously in time and frequency, allowing for an intuitive visualization of the nonlinear dynamics. The spectrogram is a windowed Fourier transform defined by

$$S(z,t,\omega) = \int_{-\infty}^{\infty} E_{\mathrm{ref}}(\tau'-\tau)E(z,\tau')\exp[-i\omega\tau']\mathrm{d}\tau'. \tag{11}$$

Here E_{ref} is an envelope of a reference pulse and E is the envelope of the field inside the fibre. Spectrograms are used below to identify features in the evolution of supercontinuum generation.

4. Supercontinuum design

The choice of fibre properties for supercontinuum generation depends on a number of factors based on the pump source selected and the desired spectral and temporal properties of the output. In what follows I describe two regimes that may be desirable, but which require quite different fibre properties. I refer to figure 4 throughout the following discussion.

4.1 *Very high average power, continuous wave, 1–2 μm supercontinuum*

In this case the desired supercontinuum process proceeds as follows [27]:

1. The pump propagates in the anomalous dispersion region, leading to modulation instability and the creation of ultra-short solitons (see figure 5a) [51–54]. For this to occur efficiently, a low anomalous dispersion and high nonlinearity are required. The modulation frequency is given by $\Delta\omega_{\mathrm{MI}} = \sqrt{(2\gamma P)/(|\beta_2|)}$, and the maximum side-band gain is simply $2\gamma P$, where P is the pump power. The modulation instability (MI) period is then simply given by $T_{\mathrm{MI}} = 2\pi/(\Delta\omega_{\mathrm{MI}})$. It can be shown that the soliton full-width half-maximum

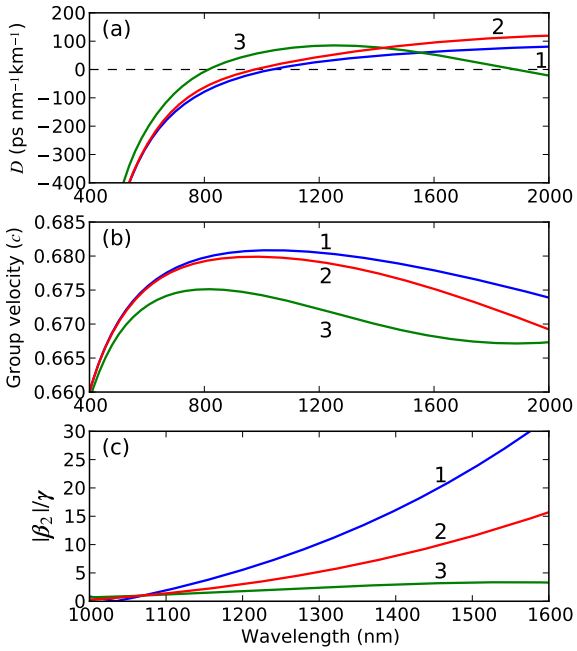

Figure 4. Some photonic crystal fibre parameters for supercontinuum generation. (**a**) Group velocity dispersion; (**b**) group velocity; (**c**) the normalized ratio $|\beta_2|/\gamma$ indicating the expected soliton broadening on red-shift. The fibres shown are: (1) denoted F1, $\Lambda = 3.4$ μm, $d/\Lambda = 0.47$; (2) denoted F2, $\Lambda = 3.5$ μm, $d/\Lambda = 0.8$; (3) denoted F3, $\Lambda = 1.7$ μm, $d/\Lambda = 0.5$.

duration is $\sim T_{\mathrm{MI}}/5$ [14,27,56], i.e. the shorter the modulation instability period, the shorter the solitons that emerge.

2. Solitons efficiently red-shift through Raman self-scattering (see figure 5b) [47,48]. In this process, the higher frequency components of a soliton cause gain, through Raman scattering, to the lower frequency components. This leads to a net frequency down-shift, but because of the inherent stability of fundamental solitons, the process is usually adiabatic. The rate of soliton frequency shift through a fibre is given approximately by $\partial_z \omega \propto -|\beta_2|/\tau_0^4$. The strong dependence on the soliton duration reflects the requirement for the soliton bandwidth to be a significant fraction of the Raman gain spectrum, for self-scattering to occur, and the soliton power dependence of the Raman gain. The majority of the spectral expansion to the long wavelength side of a supercontinuum is caused by this process or the closely related process of cross-Raman scattering between temporally colliding solitons [56–58].

The initial stage of the supercontinuum development in this case can be fulfilled with most fibres with relatively low anomalous dispersion and reasonable nonlinearity at the pump wavelength chosen. The overall continuum dynamics however, are governed by the second stage, and this has stricter requirements. As the rate of soliton self-frequency shift of the MI-induced solitons depends very strongly on the soliton duration, any temporal broadening (or equivalently spectral narrowing) of the solitons can halt the continuum development. For most pump/fibre conditions, the self-frequency shift is slow enough for the evolution of the soliton to be adiabatic as it moves through the changing dispersion and nonlinearity of the fibre at different wavelengths. This means that if the dispersion increases with wavelength, from the value at the pump wavelength, or the nonlinearity decreases, the soliton duration will respond as per eq. (10). To see how particular fibre parameters can affect this process, figure 4c shows the ratio $|\beta_2|/\gamma$, normalized to that ratio for each fibre at a pump wavelength of 1070 nm, for the three example fibres. It is clear that whereas fibre F1 shows a dramatic increase in this ratio, and hence one would expect the soliton continuum to be significantly limited, F3 maintains the ratio almost at a constant, as it has a second zero dispersion wavelength. Such a fibre is an optimal choice for this kind of CW supercontinuum [27].

The long wavelength extent of such a continuum is limited by third-order dispersion or a decrease in nonlinearity, as described above, high water loss [59,60] or a second zero dispersion [29,61] which causes a halt to the self-frequency shift and the creation of a long wavelength dispersive wave (see figure 5c) [62]. The optimal fibre for such a continuum is likely to be one with a carefully controlled double zero dispersion [27]. Note that these conditions are very different from those required for efficient short-wavelength generation, described below, in that the first zero dispersion wavelength needs to be far from the pump wavelength to minimize the role of third-order dispersion.

4.2 *High average power, visible spectral region supercontinuum*

In this case the desired supercontinuum process proceeds as follows [14,17]:

1. The pump propagates in the anomalous dispersion region, leading to modulation instability and the creation of ultra-short solitons like stage 1 in the previous section (see figure 5d).
2. The pump wavelength is sufficiently close to the zero dispersion wavelength for the MI-induced solitons to have significant spectral overlap with the normal dispersion region, and hence dispersive wave generation can occur leading to a build up of spectral power in the normal dispersion regime (see figure 5e) [63–67].
3. The remaining solitons begin to red-shift through Raman self-scattering, as above. While red-shifting, the solitons may trap some of the dispersive waves, leading to their blue-shift, thus forming a supercontinuum (see figure 5f) [68–72]. This is the main mechanism for the blue spectral expansion in an MI-dominated supercontinuum [14].

Stages 1 and 2 require relatively low anomalous dispersion and high nonlinearity. Stage 2, specifically requires the pump to be close to the zero dispersion wavelength. Fibres F1 and F2 in figure 4 fulfil these requirements. The short wavelength extent of such a continuum however, is limited by the shortest group velocity matched wavelength, as the process of stage 3, that of soliton trapping of dispersive waves requires the group velocity of the red-shifting soliton to match that of the short wavelength dispersive wave. The optimal photonic crystal fibre for this stage is actually quite sub-optimal for the initial MI and dispersive wave generation process, as it favours a quite short zero dispersion wavelength (around 800 nm), whereas low dispersion at the pump wavelength and good spectral overlap between the MI solitons and normal dispersion requires a longer zero dispersion wavelength (around 1000–1050 nm), and so some compromise is required. The choice depends strongly on the pump conditions:

Picosecond pump pulses. In this case the pump power is sufficiently high that relatively sub-optimal dispersion and nonlinearity at the pump wavelength can be tolerated, and the solitons are often spectrally broad enough to overlap quite far from the pump wavelength. A good choice has been found with a zero dispersion wavelength around ∼1000 nm [3], for an example, a fibre like F2 shown in figure 4. From figure 4b we see that long wavelength solitons in F2 can be matched to dispersive waves at wavelengths as short as ∼500 nm, as opposed to ∼600 nm with fibre F1. Alternatively two cascaded fibres, to optimize the separate stages of the process, can be used. In this technique, a first fibre, like F1, is chosen to be optimal for the initial MI and dispersive wave generation stages (1 and 2), and a second fibre, like F3, is used for soliton trapping of dispersive waves to shorter wavelengths (stage 3). This has been successfully demonstrated in [14,73]. The best technique, however, appears to be with the use of tapered fibres [1,2], which allows for a transition between optimal MI conditions and optimal trapping conditions, and has been shown to strongly enhance the trapping process [74].

Continuous-wave pump. In this case, a close zero dispersion wavelength is essential for getting short-wavelength generation [27,75], as the MI-induced solitons from a CW pump source are quite narrow spectrally. Therefore, of the fibre examples in figure 4, only F1 is useful, and a similar fibre has been successfully used to demonstrate some visible CW supercontinuum [76]. Tapered fibres have produced

much better results [77,78], as has extremely high power CW pumping of a fibre like F1 [5].

5. Experimental results

As examples of what can be achieved with the above considerations, in this section I provide a brief overview of some recent experimental results.

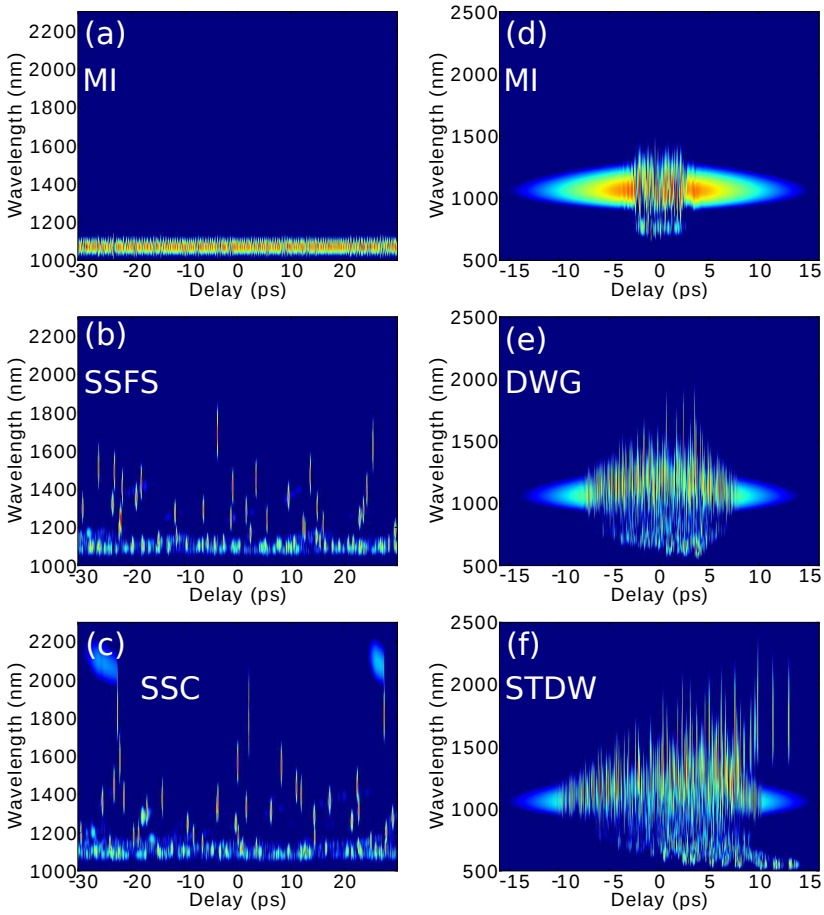

Figure 5. Spectrograms of the numerically modelled evolution of supercontinuum generation. (**a**)–(**c**) Pumping fibre F3 with 50 W CW fibre laser (**a**) 2.5 m, (**b**) 8.6 m, (**c**) 10.1 m. (**d**)–(**e**) Pumping fibre F2 with 10 kW, 10 ps pulses (**d**) 0.1 m, (**e**) 0.25 m, (**f**) 0.5 m. MI – modulation instability, SSFS – soliton self-frequency shift, DWG – dispersive wave generation, SSC – soliton shift cancellation, STDW – soliton trapping of dispersive waves.

5.1 *Very high average power, continuous wave, supercontinuum generation*

Figure 6 shows some results for continuous wave pumping. Figure 6(1) shows how pumping a fibre like F1 with low CW power creates a relatively restricted supercontinuum [79]. This is because the solitons generated at the pump wavelength cannot efficiently self-frequency shift because they temporally broaden due to increasing dispersion at longer wavelengths, as shown in figure 4c. In contrast, figure 6(2) shows how using a double zero-dispersion wavelength PCF, like F3, enables a broad and flat supercontinuum to longer wavelengths to be created, as the solitons do not broaden because the dispersion is held quite constant over the spectral range, as shown in figure 4c [29]. In this case the continuum expansion is stopped by the second zero dispersion wavelength cancelling the soliton self-frequency shift [62]. Finally, figure 6(4) shows how a continuous wave visible supercontinuum can be generated, with very high average spectral power, by pumping a fibre like F1 with very high average power (220 W).

5.2 *High average power, picosecond pumped visible spectral region supercontinuum generation*

Figure 7 shows some examples of supercontinua generated with picosecond pumping of PCFs. The pump parameters were all approximately the same for all cases, with ∼8 ps pulses, ∼50 MHz repetition rate and ∼5 W of average pump power. Figure 7(1) shows the results for pumping a fibre similar to F1 in figure 4 [22]. A supercontinuum from around ∼600 nm to longer wavelengths is produced. The short wavelength limit is caused by a lack of group velocity matching between the

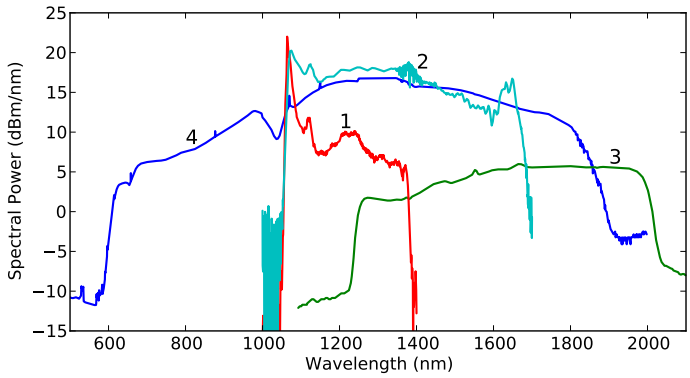

Figure 6. Examples of the extent of spectral power achieved with continuous wave supercontinuum generation: (1) using 100 m of PCF like F1, with a 10 W Yb fibre laser [80]; (2) using 25 m of PCF like F3, with a 50 W Yb fibre laser [29]; (3) using 600 m of highly nonlinear conventional fibre with a 10 W Er fibre laser [81]; (4) using 50 m of PCF like F1, with a 220 W Yb fibre laser [5].

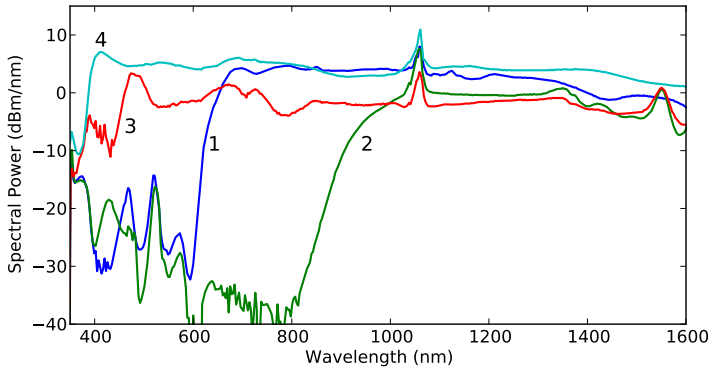

Figure 7. Examples of the extent of spectral power achieved with ∼8 ps, 50 MHz, 5 W MOPFA pumped supercontinuum generation: (1) using ∼1 m of PCF similar to F1, after [22]; (2) 10 m of PCF similar to F3, after [73]; (3) using a cascade of 1 m of PCF like F1 and 10 m of PCF like F3, after [73]; (4) using 1 m of a tapered PCF, after [1,2].

red-shifting solitons and the dispersive wave components. Figure 7(2) shows the results of directly pumping a fibre like F3 in figure 4 [73]. In this case no short wavelength generation is achieved, because the zero dispersion wavelength is too far from the pump wavelength for significant spectral overlap between the MI-induced solitons and dispersive wave phase-matched wavelengths (as described above). Instead a Raman-soliton continuum is formed to longer wavelengths. Figure 7(3) shows the results of pumping a fibre like F3 with the output of the continuum shown as figure 7(1) [73]. This produced a shorter wavelength continuum extension, because the dispersive waves efficiently excited in the first stage (figure 7(1)) can now be group velocity matched to shorter wavelengths in fibre F3 (compare F1 and F3 in figure 4b). Finally figure 7(4) shows how the use of a tapered PCF, between the properties of F1 and F3, can create a supercontinuum that is very flat across the visible spectrum, with high spectral power, and also extends to below 400 nm [1].

6. Conclusion

The experimental requirements to generate high average power supercontinua have been described, including a detailed description of high power, fibre-based pump sources, and the photonic crystal fibres used as the nonlinear medium. In addition, a widely used numerical model has been detailed with some guidelines for its solution. Using such techniques, some numerical results were presented in conjunction with detailed qualitative guidelines for the design of a number of specific supercontinuum outcomes. Finally, I presented experimental results showing how very high, mW/nm scale, average spectral powers can be achieved across the visible spectrum, and how orders of magnitude higher spectral powers can be achieved in the near-infrared with continuous-wave pump sources.

Acknowledgements

The author wishes to thank his current and past colleagues J R Taylor, S V Popov, A B Rulkov, B A Cumberland, R E Kennedy, E J R Kelleher and B Chapman, for entertaining and illuminating discussions and their patience. The author would also like to thank J M Dudley, J C Knight, A Kudlinski and J Stone for useful discussions and collaborations. This work has been partially supported by the UK Engineering and Physical Sciences Research Council, and the author is currently supported by an Imperial College Junior Research Fellowship.

References

[1] A Kudlinski, A K George, J C Knight, J C Travers, A B Rulkov, S V Popov and J R Taylor, *Opt. Express* **14**, 5715 (2006)
[2] J C Travers, A B Rulkov, S V Popov, J R Taylor, A Kudlinski, A K George and J C Knight, *Conference on Lasers and Electro-Optics* (Optical Society of America, Baltimore, MD, USA, 2007) p. JTuB2
[3] J M Stone and J C Knight, *Opt. Express* **16**, 2670 (2008)
[4] C Xia, M Kumar, O P Kulkarni, M N Islam Jr, Fred L Terry, M J Freeman, M Poulain and G Mazé, *Opt. Lett.* **31**, 2553 (2006)
[5] J C Travers, A B Rulkov, B A Cumberland, S V Popov and J R Taylor, *Opt. Express* **16**, 14435 (2008)
[6] D R Solli, C Ropers, P Koonath and B Jalali, *Nature* **450**, 1054 (2007)
[7] D R Solli, C Ropers and B Jalali, *Phys. Rev. Lett.* **101**, 23 (2008)
[8] J M Dudley, G Genty and B J Eggleton, *Opt. Express* **16**, 3644 (2008)
[9] M Erkintalo, G Genty and J M Dudley, *The Euro. Phys. J. – Special Topics* **185**, 135 (2010)
[10] V Ruban, Y Kodama, M Ruderman, J Dudley, R Grimshaw, P V E McClintock, M Onorato, C Kharif, E Pelinovsky, T Soomere, G Lindgren, N Akhmediev, A Slunyaev, D Solli, C Ropers, B Jalali, F Dias and A Osborne, *The Euro. Phys. J. – Special Topics* **185**, 5 (2010)
[11] T G Philbin, C Kuklewicz, S Robertson, S Hill, F Konig and U Leonhardt, *Science* **319**, 1367 (2008)
[12] B Barviau, B Kibler, S Coen and A Picozzi, *Opt. Lett.* **33**, 2833 (2008)
[13] G Genty, S Coen and J M Dudley, *J. Opt. Soc. Am.* **B24**, 1771 (2007)
[14] J C Travers, *J. Opt.* **12** (2010)
[15] G P Agrawal, *Nonlinear fiber optics* 4th ed. (Academic Press, San Diego, 2007)
[16] J R Taylor, ed., *Optical Solitons: Theory and experiment* 1st ed. (Cambridge University Press, Cambridge, 1992)
[17] J M Dudley and J R Taylor, eds., *Supercontinuum generation in optical fibers*, 1st ed. (Cambridge University Press, Cambridge, 2010)
[18] R R Alfano, ed., *The supercontinuum laser source* (Springer, New York, 2006)
[19] J M Dudley, G Genty and S Coen, *Rev. Mod. Phys.* **78**, 1135 (2006)
[20] D V Skryabin and A V Gorbach, *Rev. Mod. Phys.* **82**, 1287 (2010)
[21] K K Chen, S ul Alam, J H V. Price, J R Hayes, D Lin, A. Malinowski, C Codemard, D Ghosh, M Pal, S K Bhadra and D J Richardson, *Opt. Express* **18**, 5426 (2010)
[22] A Rulkov, M Vyatkin, S Popov, J Taylor and V Gapontsev, *Opt. Express* **13**, 377 (2005)

[23] E A De Souza, C E Soccolich, W Pleibel, R H Stolen, J R Simpson and D J DiGiovanni, *Electron. Lett.* **29**, 447 (1993)
[24] S Y Set, H Yaguchi, Y Tanaka and M Jablonski, *IEEE J. Sel. Top. Quantum Electron.* **10**, 137 (2004)
[25] S Yamashita, Y Inoue, S Maruyama, Y Murakami, H Yaguchi, M Jablonski and S Y Set, *Opt. Lett.* **29**, 1581 (2004)
[26] J C Travers, S V Popov and J R Taylor, *Conference on Lasers and Electro-Optics* (2008) p. CMT3
[27] J C Travers, in: *Supercontinuum generation in optical fibers* edited by J M Dudley and J R Taylor (Cambridge University Press, 2010) Ch. 8
[28] C J S de Matos, S V Popov and J R Taylor, *Appl. Phys. Lett.* **85**, 2706 (2004)
[29] B A Cumberland, J C Travers, S V Popov and J R Taylor, *Opt. Express* **16**, 5954 (2008)
[30] J C Knight, T A Birks, P S Russell and D M Atkin, *Opt. Lett.* **21**, 1547 (1996)
[31] J C Knight, *Nature (London)* **424**, 847 (2003)
[32] P S J Russell, *Science* **299**, 358 (2003)
[33] P S J Russell, *J. Lightwave Technol.* **24**, 4729 (Dec 2006)
[34] J C Knight, J Arriaga, T A Birks, A Ortigosa-Blanch, W J Wadsworth and P S J Russell, *IEEE Photonic. Tech. L.* **12**, 807 (2000)
[35] W Reeves, J C Knight, P S J Russell and P Roberts, *Opt. Express* **10**, 609 (2002)
[36] K Saitoh and M Koshiba, *J. Lightwave Technol.* **23**, 3580 (2005)
[37] J K Ranka, R S Windeler and A J Stentz, *Opt. Lett.* **25**, 796 (2000)
[38] K J Blow and D Wood, *IEEE J. Quantum Electron.* **25**, 2665 (1989)
[39] P V Mamyshev and S V Chernikov, *Opt. Lett.* **15**, 1076 (1990)
[40] P L Francois, *J. Opt. Soc. Am.* **B8**, 276 (1991)
[41] J Lægsgaard, *Opt. Express* **15**, 16110 (2007)
[42] R H Stolen, J P Gordon, W J Tomlinson and H A Haus, *J. Opt. Soc. Am.* **B6**, 1159 (1989)
[43] D Hollenbeck and C D Cantrell, *J. Opt. Soc. Am.* **B19**, 2886 (2002)
[44] Q Lin and G P Agrawal, *Opt. Lett.* **31**, 3086 (2006)
[45] Velko P Tzolov, M Fontaine, N Godbout and S Lacroix, *Opt. Lett.* **20**, 456 (1995)
[46] V E Zakharov and A B Shabat, *JETP Lett.* **34**, 62 (1972)
[47] E M Dianov, A Y Karasik, P V Mamyshev, A M Prokhorov, V N Serkin, M F Stelmakh and A A Fomichev, *JETP Lett.* **41**, 294 (1985)
[48] J P Gordon, *Opt. Lett.* **11**, 662 (1986)
[49] S G Johnson and J D Joannopoulos, *Opt. Express* **8**, 173 (2001)
[50] J C Travers, M H Frosz and J M Dudley, in: *Supercontinuum generation in optical fibers* edited by J M Dudley and J R Taylor (Cambridge University Press, 2010) Ch. 3
[51] V E Zakharov and L A Ostrovsky, *Physica D: Nonlinear Phenomena* **238**, 540 (2009)
[52] A Hasegawa and W F Brinkman, *IEEE J. Quantum Electron.* **16**, 694 (1980)
[53] K Tai, A Hasegawa and A Tomita, *Phys. Rev. Lett.* **56**, 135 (1986)
[54] Hiroki Itoh, Gillian M Davis and Shoichi Sudo, *Opt. Lett.* **14**, 1368 (1989)
[55] E M Dianov, A B Grudinin, A M Prokhorov and V N Serkin, in: *Optical solitons: Theory and experiment* edited by J R Taylor (Cambridge University Press, 1992) Ch. 7, p. 197
[56] M N Islam, G Sucha, I Bar-Joseph, M Wegener, J P Gordon and D S Chemla, *J. Opt. Soc. Am.* **B6**, 1149 (1989)
[57] M H Frosz, O Bang and A Bjarklev, *Opt. Express* **14**, 9391 (2006)

[58] N Korneev, E A Kuzin, B Ibarra-Escamilla and M B J A Flores-Rosas, *Opt. Express* **16**, 2636 (2008)
[59] J C Travers, S V Popov and J R Taylor, *Opt. Lett.* **30**, 3132 (2005)
[60] N J Traynor, A Monteville, L Provino, D Landais, O Le Goffic, T N Nguyen, T Chartier, D Tregoat and J C Travers, *Fiber Integrated Opt.* **28**, 51 (2009)
[61] A Kudlinski, G Bouwmans, Y Quiquempois and A Mussot, *Appl. Phys. Lett.* **92**, 14 (2008)
[62] F Biancalana, D V Skryabin and A V Yulin, *Phys. Rev.* **E70**, 016615 (2004)
[63] P K A Wai, C R Menyuk, Y C Lee and H H Chen, *Opt. Lett.* **11**, 464 (1986)
[64] V I Karpman, *Phys. Rev.* **E47**, 2073 (1993)
[65] N Akhmediev and M Karlsson, *Phys. Rev.* **A51**, 2602 (1995)
[66] A V Gorbach, D V Skryabin, J M Stone and J C Knight, *Opt. Express* **14**, 9854 (2006)
[67] D V Skryabin and A V Yulin, *Phys. Rev.* **E72**, 016619 (2005)
[68] P Beaud, W Hodel, B Zysset and H Weber, *IEEE J. Quantum Electron.* **23**, 1938 (1987)
[69] N Nishizawa and T Goto, *Opt. Express* **10**, 1151 (2002)
[70] G Genty, M Lehtonen and H Ludvigsen, *Opt. Express* **12**, 4614 (2004)
[71] A V Gorbach and D V Skryabin, *Nat. Phot.* **1**, 653 (2007)
[72] A V Gorbach and D V Skryabin, *Phys. Rev.* **A76**, 053803 (2007)
[73] J C Travers, S V Popov and J R Taylor, *Opt. Lett.* **30**, 3132 (2005)
[74] J C Travers and J R Taylor, *Opt. Lett.* **34**, 115 (2009)
[75] J C Travers, *Opt. Express* **17**, 1502 (2009)
[76] B A Cumberland, J C Travers, S V Popov and J R Taylor, *Opt. Lett.* **33**, 2122 (2008)
[77] A Kudlinski and A Mussot, *Opt. Lett.* **33**, 2407 (2008)
[78] A Mussot and A Kudlinski, *Electron. Lett.* **45**, 29 (2009)
[79] A V Avdokhin, S V Popov and J R Taylor, *Opt. Lett.* **28**, 1353 (2003)
[80] S V Popov, P A Champert, M A Solodyankin and J R Taylor, *Proceedings OSA Annual Meeting*, p. 117 (2002)